Article ID: 1000-7032(2022)03-0359-12

Bipolar Fluorenylcarbazole-based Host Materials for Efficient Red Phosphorescent Organic Light-emitting Diodes

LING Qian-kun[1], DONG Bi-zheng[1], CHEN Zhi-kuan[2*], WANG Hua[1*], WEI Ting-wei[2], LI Xiang-zhi[2], ZHAO Bo[2], LI Tian-bao[1*], CHEN Fei[2,3]

(1. *Key Laboratory of Interface Science and Engineering in Advanced Materials, Ministry of Education, Taiyuan University of Technology, Taiyuan* 030024, *China*;
2. *Ningbo Research Institute of Northwestern Polytechnical University, Ningbo* 315199, *China*;
3. *Department of Chemical and Environmental Engineering, The University of Nottingham Ningbo China, Ningbo* 315199, *China*)
* *Corresponding Authors, E-mail: zkchen@lumilan.cn; wanghua001@tyut.edu.cn; litianbao@tyut.edu.cn*

Abstract: Achieving high-efficiency red phosphorescent organic light-emitting diodes (PhOLEDs) is still a challenge, which is largely related to the host material used in device fabrication. Two new bipolar hosts, 2-(9*H*-carbazol-9-yl)-7,7-dimethyl-5-(4-phenylquinazolin-2-yl)-5,7-dihydroindeno[2,1-b]carbazole (FC-CZ-PQZ) and 2-(4-(9*H*-carbazol-9-yl) phenyl)-7,7-dimethyl-5-(4-phenylquinazolin-2-yl)-5,7-dihydroindeno[2,1-b]carbazole (FC-BCz-PQZ), were designed and synthesised as host materials to fabricate red PhOLEDs. The two compounds exhibited excellent physical properties with high thermal stabilities and balanced charge transport. FC-BCz-PQZ has a better bipolar carrier transport compared to FC-CZ-PQZ. FC-BCz-PQZ-based device demonstrated good electroluminescence performance with the maximum current efficiency, power efficiency and external quantum efficiency of 13.5 cd/A, 14.2 lm/W and 14.8%, respectively, suggesting its promising application as a host material for red PhOLEDs.

Key words: fluorenylcarbazole; quinazoline; red PhOLEDs; bipolar hosts
CLC number: O482.31 **Document code**: A **DOI**: 10.37188/CJL.20210397

用于高效红色磷光有机发光二极管的双极性芴基咔唑基主体材料

凌乾坤[1], 董必正[1], 陈志宽[2*], 王 华[1*], 魏定纬[2], 李祥智[2], 赵 波[2], 李天保[1*], 陈 飞[2,3]

(1. 太原理工大学 新材料界面科学与工程教育部重点实验室, 山西 太原 030024;
2. 西北工业大学 宁波研究院, 浙江 宁波 315199; 3. 宁波诺丁汉大学 化学环境工程系, 浙江 宁波 315199)

摘要: 为提高有机发光二极管的发光效率,设计合成了两种新的红光磷光双极性主体材料 FC-CZ-PQZ 和 FC-BCz-PQZ,两种材料均表现出优秀的光物理性能、较高热稳定能力和平衡的载流子传输能力,FC-BCz-PQZ 表现最佳,与 FC-Cz-PQZ 相比,FC-BCz-PQZ 的热稳定能力更强、载流子传输平衡性更好。以 FC-CZ-PQZ 和 FC-BCz-PQZ 为主体,制备了红色 PhOLEDs,FC-BCz-PQZ 表现出了较高的电致发光性能,电流效率、功率效率和最大外量子效率分别为 13.5 cd/A、14.2 lm/W 和 14.8%, 说明 FC-BCz-PQZ 有潜力成为红光 PhOLED 主体材料。

关 键 词: 芴基咔唑; 喹唑啉; 红光 PhOLEDs; 双极性主体

收稿日期: 2021-12-16; **修订日期**: 2022-01-07
基金项目: 国家自然科学基金(62074109,21875106)资助项目
Supported by National Natural Scientific Foundation of China(62074109,21875106)

1 Introduction

Since the discovery of organic light-emitting devices (OLEDs) by Tang *et al.*[1], this technology has been eventually applied because of its low power consumption, high brightness, flexible and wide view angle[2-3]. Unfortunately, the efficiency of red OLEDs is not sufficient to date. Therefore, numerous materials and device structures have been designed for improving the device performance. The red phosphorescent materials of iridium(Ⅲ) complexes are widely applied as emitters because they can harvest both singlet and triplet excitons to achieve 100% internal quantum efficiency[4-6]. However, iridium(Ⅲ) complexes are usually long-lived at their triplet excitons during the relaxation processes, resulting in remarkable roll-off due to triplet-triplet annihilation(TT-A) and exciton quenching. To solve this issue, iridium(Ⅲ) complexes have been used as low-concentration dopants along with appropriate host materials in the emitting layer[7-11]. The bipolar host materials with balanced charge mobility have recently acquired wide research attention. An adequate bipolar host material for phosphorescent OLEDs(PhOLEDs) has to satisfy the following requirements: good thermal stability, highest occupied molecular orbital(HOMO)/lowest unoccupied molecular orbital(LUMO) levels for charge injections, high triplet energy and high charge mobilities[12-16].

In recent years, red phosphorescent host materials have been rapidly developed[17-34]. Carbazole is a frequently used molecular fragment because of its several excellent properties, including high triplet energy level and chemical stability, which make carbazole-containing molecules as hole-transport materials in OLEDs[35-36]. Besides, quinoxaline derivatives are widely used as electron-transport materials due to their high electron mobility[28,37-38]. Hu designed four host materials with quinoxaline as the acceptor, in which the maximum external quantum efficiency (EQE) was only 12.2% due to their low electron mobility[39]. Fan designed a bipolar host material for high-efficiency red PhOLEDs, which was composed of two 6*H*-indolo[2,3-b]quinoxaline units bridged by tetraphenylsilane linkage, which exhibited EQE exceeding 20%[38]. In spite of these reports, it is still a challenge to design ideal host materials with a quinoxaline unit for red PhOLEDs with high efficiencies. Quinazoline is similar in structure to quinoxaline and has high electron confinement ability, thus, it has the potential to facilitate the A unit of D-A type materials. Li and his coworkers used quinazoline as the A unit to construct efficient quinazoline-based thermally activated delayed fluorescence materials, and the devices using these materials achieved high EQE of up to 20%[38]. In this paper, the quinazoline derivative 4-phenylquinazoline(PQZ) was utilised as the A unit to facilitate electron mobility.

Taking the advantage of the carbazole and quinazoline, two host materials, namely, 9*H*-carbazol-9-yl)-7,7-dimethyl-5-(4-phenylquinazolin-2-yl)-5,7-dihydroindeno[2,1-b]carbazole (FC-Cz-PQZ) and 2-(4-(9*H*-carbazol-9-yl)phenyl)-7,7-dimethyl-5-(4-phenylquinazolin-2-yl)-5,7-dihydroindeno[2,1-b]carbazole (FC-BCz-PQZ), were designed and synthesised. We introduced a quinazoline moiety as the acceptor to facilitate electron transport and phenyl rings to enhance molecular thermal stability. The structure of the carbazole is flat and easily causes intermolecular packing, whereas fluorene exhibits good rigidity. Hence, we introduced fluorenylcarbazole(FC) composed of carbazole and 9,9-dimethylfluorene as the donor to increase the thermal stability by enhancing the rigidity of the spiral structure and to avoid quenching of exciton concentration, which contribute to the improvement of luminous efficiency. Furthermore, carbazole was introduced at position 3 of FC to improve hole mobility. Besides, bridge benzene was introduced between carbazole and FC to investigate the effect of benzene on the material properties. Experimental results showed that the two host materials exhibited excellent physical properties and high thermal stabilities for red PhOLEDs. The red PhOLEDs based on the host material FC-BCz-PQZ achieved good electroluminescence(EL) performance with the maximum current, power and EQE of 13.5 cd/A, 14.2 lm/W and 14.8%, respectively.

2 Experiments

2.1 Synthesis

In this work, all solvents and reagents used for the synthesis of materials, and medicines were purchased without purification. The synthetic routes are shown in Scheme 1.

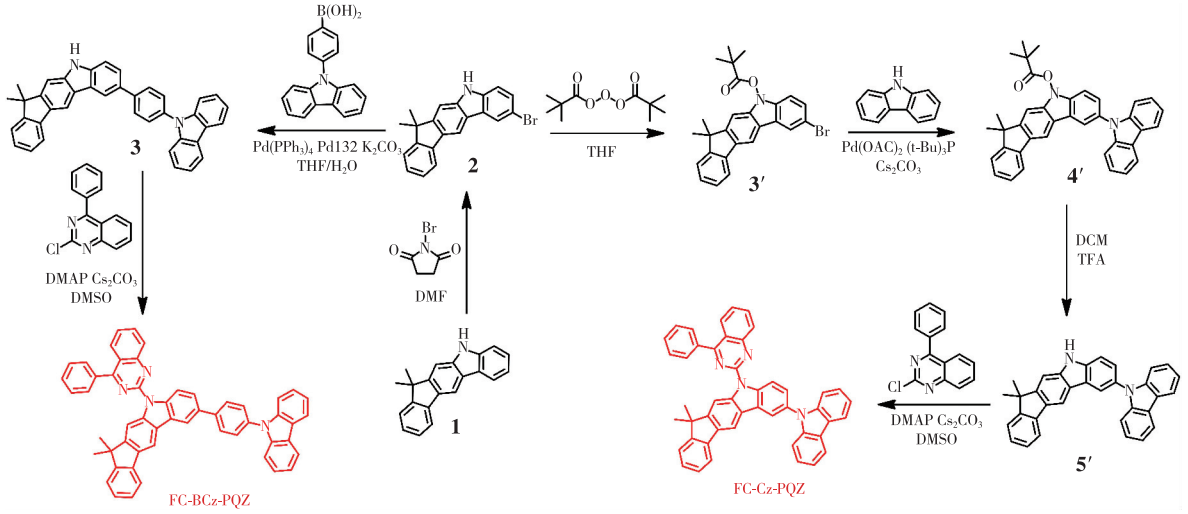

Scheme 1　Synthetic routes of FC-BCz-PQZ and FC-Cz-PQZ

2.1.1　FC-BCz-PQZ

(1) 2-Bromo-7,7-dimethyl-5,7-dihydroindeno[2,1-b]carbazole (2)

A mixture of 7,7-dimethyl-5,7-dihydroindeno[2,1-b]carbazole (10 g, 42.0 mmol) and *N*,*N*-dimethylformamide(100 mL) was placed in a 250-mL flask. Then, *N*-bromosuccinimide (6.29 g, 42.0 mmol) was dissolved in 7,7-dimethyl-5,7-dihydroindeno[2,1-b] carbazole (63 mL) and was slowly added into the mixture through a dropping funnel under nitrogen atmosphere and at a constant pressure. The reaction mixture was stirred for 30 min at 0 ℃, filtered under vacuum and washed with ethyl alcohol, affording the white solid intermediate product 2(10.6 g, yield 70%). ^{1}H NMR(500 MHz, $CDCl_3$)δ 8.32(s, 1H), 8.24(d, J = 1.7 Hz, 1H), 8.05(s, 1H), 7.82(d, J = 7.5 Hz, 1H), 7.48 (dd, J = 8.5, 1.9 Hz, 1H), 7.45 – 7.41(m, 2H), 7.37(t, J = 7.8 Hz, 1H), 7.29(t, J = 7.2 Hz, 2H), 1.55(s, 6H). ^{13}C NMR(126 MHz, DMSO) δ 153.02, 152.75, 140.45, 139.17, 138.76, 130.83, 127.42, 126.98, 126.15, 124.58, 122.60, 122.44, 120.94, 119.04, 112.87, 111.81, 110.49, 105.39, 55.95, 54.81, 46.12, 27.66, 18.47. Mass(ESI, m/z): $[M+H]^+$ calculated for $C_{21}H_{16}BrN$: 362.26, found: 362.17.

(2) 2-(4-(9*H*-Carbazol-9-yl) phenyl)-7,7-dimethyl-5,7-dihydroindeno[2,-1-b] carbazole (3)

A mixture of the intermediate product 2(10 g, 27.7 mmol), 4-(9-carbazole) phenylboric acid (7.95 g, 33.2 mmol), tetrakis (triphenylphosphine)palladium(1.61 g, 1.39 mmol), dichlorobis [di-*tert*-butyl(4-dimethylaminophenyl) phosphine] palladium(Ⅱ)(0.98 g, 139 mmol) and potassium carbonate(9.42 g, 69.25 mmol) was dissolved in a solution of tetrahydrofuran and water(100 mL, v/v = 2∶1). Then, the reaction mixture was refluxed for 3 h under nitrogen atmosphere and was extracted with CH_2Cl_2. Afterwards, the solvent was removed by vacuum, and the white solid intermediate product 3(9.72 g, 67%) was obtained and then purified by silica gel column chromatography. ^{1}H NMR (500 MHz, $CDCl_3$) δ 8.39(s, 1H), 8.38(d, J = 1.6 Hz, 1H), 8.11(d, J = 7.7 Hz, 2H), 8.04(s, 1H), 7.90 – 7.87(m, 2H), 7.78 (d, J = 7.5 Hz, 1H), 7.68 (dd, J = 8.3, 1.8 Hz, 1H), 7.62 – 7.58(m, 2H), 7.45(dd, J = 8.3, 2.7 Hz, 3H), 7.40 – 7.36(m, 4H), 7.31(dd, J = 14.8, 1.0 Hz, 1H), 7.26 – 7.20(m, 3H), 1.50(s, 6H). ^{13}C NMR(126 MHz, $CDCl_3$) δ 152.39, 152.17, 140.28, 139.97, 139.29, 138.69, 138.51, 135.05, 131.17, 130.99, 127.54, 126.37, 126.08, 125.32, 124.93, 123.95,

123.26, 122.36, 121.91, 121.55, 119.29, 118.86, 118.27, 117.74, 110.41, 109.99, 108.89, 104.07, 45.64, 26.99. Mass(ESI, *m/z*): $[M+H]^+$ calculated for $C_{39}H_{30}N_2$: 525.23, found: 525.39.

(3) FC-BCz-PQZ

A mixture of the intermediate product 3 (9 g, 17.2 mmol), 2-chloro-4-phenylquinazoline (4.95 g, 20.64 mmol), 4-dimethylaminopyridine (2.10 g, 17.2 mmol) and cesium carbonate (11.2 g, 34.4 mmol) was dissolved in dimethyl sulfoxide (90 mL). Then, the reaction mixture was refluxed for 2 h under nitrogen atmosphere and added with water. Afterwards, the reaction mixture was filtered under vacuum and washed with ethyl alcohol, affording the yellow solid FC-BCz-PQZ (12.9 g, 69%). ^{1}H NMR (500 MHz, $CDCl_3$) δ 9.24 (s, 1H), 9.20 (d, J = 8.6 Hz, 1H), 8.45 (s, 1H), 8.44 (d, J = 1.7 Hz, 1H), 8.22 – 8.15 (m, 4H), 8.04 – 8.01 (m, 2H), 8.01 – 7.97 (m, 2H), 7.94 – 7.91 (m, 1H), 7.88 (d, J = 7.4 Hz, 1H), 7.83 (dd, J = 8.6, 1.9 Hz, 1H), 7.70 – 7.65 (m, 5H), 7.54 – 7.50 (m, 3H), 7.49 (d, J = 7.3 Hz, 1H), 7.47 – 7.43 (m, 2H), 7.40 (td, J = 7.4, 0.9 Hz, 1H), 7.34 – 7.29 (m, 3H), 1.62 (s, 6H). ^{13}C NMR (126 MHz, $CDCl_3$) δ 169.63, 155.32, 153.82, 153.46, 152.77, 140.96, 140.83, 140.17, 139.61, 139.46, 137.20, 136.33, 134.32, 134.26, 134.21, 130.41, 130.28, 128.72, 128.58, 128.04, 127.37, 127.31, 127.09, 126.77, 126.67, 125.95, 125.90, 125.45, 125.42, 123.40, 122.65, 120.31, 120.21, 119.90, 119.66, 117.74, 117.14, 111.55, 110.54, 109.91, 47.02, 27.99. Mass(ESI, *m/z*): $[M+H]^+$ calculated for $C_{53}H_{38}N_4$: 728.88, found: 728.54. Anal. Calcd for $C_{53}H_{36}N_4$ (%): C, 87.33; H, 4.98; N, 7.69. Found: C, 87.36; H, 4.94; N, 7.67.

2.1.2 FC-Cz-PQZ

(1) 2-Bromo-7,7-dimethylindeno[2,1-b]carbazol-5(7*H*)-ylpivalate (3′)

The intermediate product 2 (10 g, 27.7 mmol), 4-dimethylaminopyridine (5.1 g, 41.1 mmol) and tetrahydrofuran were thoroughly mixed in a 500-mL flask under nitrogen atmosphere. Using a dropping funnel, di-*tert*-butyl pyrocarbonate (9.1 g, 41.6 mmol) was slowly added to the flask at room temperature and constant pressure. Then, water was added into the mixture and filtered under vacuum, affording a white solid product (10.9 g, 85%). ^{1}H NMR (500 MHz, $CDCl_3$) δ 8.39 (s, 1H), 8.17 (s, 1H), 8.15 – 8.10 (m, 2H), 7.80 (d, J = 7.4 Hz, 1H), 7.52 (dd, J = 8.8, 2.0 Hz, 1H), 7.46 (d, J = 7.2 Hz, 1H), 7.38 (td, J = 7.4, 1.1 Hz, 1H), 7.32 (td, J = 7.4, 1.0 Hz, 1H), 1.78 (s, 9H), 1.57 (s, 6H). ^{13}C NMR (126 MHz, $CDCl_3$) δ 154.45, 153.73, 150.81, 138.74, 137.52, 135.09, 129.32, 127.84, 127.14, 127.10, 124.08, 122.68, 122.25, 119.81, 117.77, 116.15, 111.06, 110.64, 84.29, 53.41, 47.10, 28.38, 27.76. Mass(ESI, *m/z*): $[M+H]^+$ calculated for $C_{26}H_{24}BrNO_2$: 463.10, found: 463.45.

(2) 2-(9*H*-Carbazol-9-yl)-7,7-dimethylindeno[2,1-b]carbazol-5(7*H*)-ylpivalate (4′)

The intermediate product 3′ (10 g, 21.7 mmol), palladium acetate (0.26 g, 1.1 mmol), cesium carbonate (17.7 g, 54.3 mmol) and xylene (100 mL) were thoroughly mixed in a 250-mL flask under nitrogen atmosphere and then heated in an oil bath at 140 ℃ for 8 h with vigorous stirring. The crude product was purified by silica gel column chromatography, affording a white solid product (5.95, 50%). ^{1}H NMR (500 MHz, $CDCl_3$) δ 8.35 (s, 1H), 8.27 (d, J = 1.8 Hz, 1H), 8.24 (s, 1H), 8.20 (d, J = 7.8 Hz, 2H), 7.78 (d, J = 7.5 Hz, 1H), 7.61 (t, J = 8.1 Hz, 1H), 7.55 – 7.52 (m, 1H), 7.51 (s, 1H), 7.45 (d, J = 7.4 Hz, 1H), 7.43 – 7.39 (m, 3H), 7.37 – 7.33 (m, 2H), 7.32 – 7.27 (m, 3H), 7.26 (s, 1H), 1.58 (s, 6H). ^{13}C NMR (126 MHz, DMSO) δ 153.47, 153.33, 141.72, 141.40, 139.82, 131.31, 128.31, 127.52, 126.65, 126.59, 124.74, 124.21, 123.15, 122.90, 122.30, 120.92, 120.09, 119.58, 119.32, 112.73, 112.55, 110.17, 106.00, 55.37, 46.71, 28.29. Mass(ESI, *m/z*): $[M+H]^+$ calculated for $C_{38}H_{32}N_2O_2$: 549.25, found: 549.40.

(3) 2-(9*H*-Carbazol-9-yl)-7,7-dimethyl-5,7-dihydroindeno[2,1-b]carbazole (5′)

The intermediate product 4′ (5 g, 9.12 mmol) and methylene chloride (50 mL) were thoroughly mixed in a 100 mL flask under nitrogen atmosphere. Using a dropping funnel, trifluoroacetic acid (10 mL) was slowly

added to the flask at room temperature and constant pressure, affording a white solid product (2.86 g, 70%). ^{1}H NMR (500 MHz, $CDCl_3$) δ 8.42 (d, J = 8.9 Hz, 2H), 8.16 (s, 1H), 8.14 – 8.07 (m, 3H), 7.69 (d, J = 7.3 Hz, 1H), 7.54 (d, J = 8.7 Hz, 1H), 7.38 – 7.32 (m, 4H), 7.25 – 7.22 (m, 3H), 7.16 (s, 2H), 1.76 (s, 9H), 1.52 (s, 6H). ^{13}C NMR (126 MHz, $CDCl_3$) δ 153.54, 152.80, 150.01, 140.54, 138.25, 137.79, 136.82, 134.22, 131.86, 126.45, 126.14, 126.09, 124.95, 124.83, 124.80, 123.74, 122.33, 121.65, 119.32, 119.29, 118.83, 118.80, 118.42, 117.28, 116.55, 110.21, 109.75, 109.53, 108.78, 83.36, 46.15, 27.46, 26.79. Mass (ESI, m/z): $[M+H]^+$ calculated for $C_{38}H_{32}N_2O_2$: 449.20, found: 449.35.

(4) FC-Cz-PQZ

The intermediate product 5′ (2 g, 3.07 mmol), 2-chloro-4-phenylquinazoline (0.88 g, 3.68 mmol), 4-dimethylaminopyridine (0.37 g, 3.07 mmol), cesium carbonate (2 g, 6.14 mmol) and dimethyl sulfoxide (20 mL) were thoroughly mixed in a 100-mL flask under nitrogen atmosphere and then heated in an oil bath at 120 ℃ for 1 h with vigorous stirring, affording a yellow solid product (1.38 g, 69%). ^{1}H NMR (500 MHz, $CDCl_3$) δ (10^{-6}) 9.32 (d, J = 8.8 Hz, 1H), 9.27 (s, 1H), 8.36 (s, 1H), 8.32 (d, J = 2.1 Hz, 1H), 8.27 – 8.19 (m, 4H), 8.08 – 8.04 (m, 2H), 8.00 – 7.95 (m, 1H), 7.81 (d, J = 7.4 Hz, 1H), 7.72 – 7.67 (m, 4H), 7.60 – 7.56 (m, 1H), 7.50 (dd, J = 11.7, 7.8 Hz, 3H), 7.46 – 7.42 (m, 2H), 7.39 – 7.35 (m, 1H), 7.32 (t, J = 7.2 Hz, 3H), 1.63 (s, 6H). ^{13}C NMR (126 MHz, $CDCl_3$) δ (10^{-6}) 169.92, 155.30, 153.92, 153.77, 152.78, 141.68, 140.30, 139.27, 138.95, 137.16, 134.46, 131.95, 130.53, 130.28, 128.80, 128.09, 127.43, 127.14, 126.79, 126.15, 125.92, 125.47, 124.86, 123.24, 122.66, 120.38, 119.75, 118.19, 117.83, 111.59, 110.74, 109.98, 47.08, 28.00. Mass (ESI, m/z): $[M+H]^+$ calculated for $C_{47}H_{32}N_4$: 653.37, found: 653.27. Anal. Calcd for $C_{47}H_{32}N_4$ (%): C, 86.48; H, 4.94; N, 8.58. Found: C, 86.36; H, 4.63; N, 8.47.

2.2 Measurements and Characterisations

^{1}H NMR and ^{13}C NMR spectra were recorded on a Bruker AM 500 spectrometer. Molecular mass was measured using a Waters LCT Premier XE spectrometer. Thermogravimetric analysis (TGA) and differential scanning calorimetry (DSC) were carried out using a TGA5500 instrument at a heating rate of 10 ℃/min to 700 ℃/min and a DSC 2500 instrument under nitrogen atmosphere, respectively. UV-visible absorption spectra were recorded on a TU-1810 spectrophotometer with baseline correction. Photoluminescence (PL) spectra were recorded on an F-4600 fluorescence spectrophotometer. The energy levels of the materials were determined by the ionization photoelectron spectrometer (IPS).

2.3 Device Fabrication

An indium tin oxide (ITO)-glass substrate was cleaned using detergent, deionised water and ethanol in this order. Then, it was treated with oxygen (O_2) plasma before loading into a 10-source evaporator with a base pressure of 5.0×10^{-4} Pa for device fabrication. Organic layers were deposited on the ITO-glass substrate by thermal evaporation.

3 Results and Discussion

3.1 Thermal Properties

The ideal thermal stability of organic light-emitting materials is vital for the better lifetime of OLEDs. Thus, the thermal properties of the two materials were investigated by TGA and DSC. As represented in Fig. 1 and Tab. 1, FC-BCz-PQZ and FC-Cz-PQZ exhibited high thermal decomposition temperature of 480 ℃ and 445 ℃, respectively, suggesting their good thermal stability. It was worth noting that two compounds showed similar endothermic glass transition temperature (T_g) of 173 ℃ and 169 ℃ for FC-BCz-PQZ and FC-Cz-PQZ, respectively, which were higher than that of the widely used 4,4′-bis (*N*-carbazolyl)-1,1′-biphenyl (CBP) host material. From these results, FC-BCz-PQZ with the bridge benzene was more thermally stable than FC-Cz-PQZ due to its large van der Waals forces, originating from more electron delocalisation. Such excellent thermal stability was favourable to form stable film surface morphology[39].

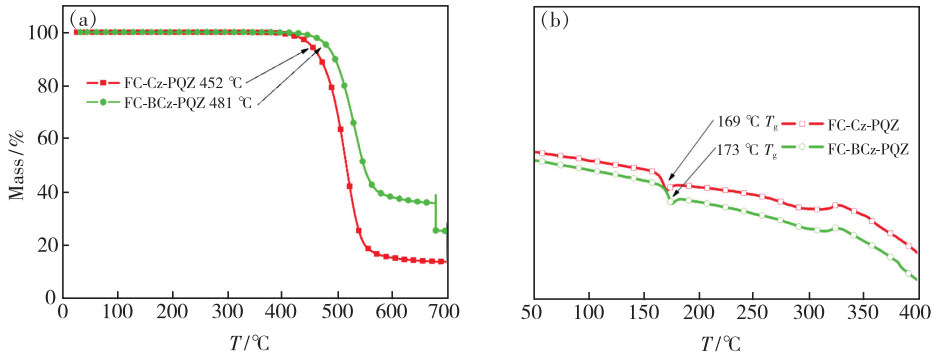

Fig. 1 TGA(a) and DSC(b) curves of FC-Cz-PQZ and FC-BCz-PQZ

Tab. 1 Physical properties of FC-Cz-PQZ and FC-BCz-PQZ

Compound	λ_{abs}[a]/nm	λ_{PL}[a]/nm	λ_{abs}[b]/nm	λ_{PL}[b]/nm	E_T[c]/eV	E_g[d]/eV	HOMO/LUMO/eV	TGA/DSC[e]/℃
FC-Cz-PQZ	321	501	319	471	2.58	3.03	−5.75/−2.72	445/165
FC-BCz-PQZ	322	506	319	491	2.57	2.93	−5.68/−2.75	480/173

[a] Measured in toluene solution. [b] Measured in the neat film. [c] Measured in toluene solution. [d] Obtained from the intersection of absorption and emission spectra. [e] From TGA and DSC measurements.

3.2 Photophysical Properties

The UV-visible absorption and emission spectra of FC-Cz-PQZ and FC-BCz-PQZ in toluene solution and in neat films at room temperature are shown in Fig. 2. The detailed data are also summarised in Tab. 1. FC-Cz-PQZ and FC-BCz-PQZ both exhibited strong absorption peaks at around 320 nm that are assigned to the π-π* transition of molecules, additional absorption peaks at 350 nm that are attributed to the n-π* transition of the carbazole moiety and weak absorption bands at 365 – 425 nm that are attributed to the intramolecular charge transfer effect of molecules. The absorption spectra of FC-Cz-PQZ and FC-BCz-PQZ displayed similar patterns, suggesting that the bridge benzene has no effect on the ground state.

The maximum emission peaks of FC-Cz-PQZ and FC-BCz-PQZ in toluene solution were observed at 501 nm and 506 nm, respectively. Compared with FC-Cz-PQZ, the emission of FC-BCz-PQZ displayed a redshift of 5 nm due to the bridge benzene extended conjugation between carbazole and FC. It was noteworthy that the emission peaks of FC-Cz-PQZ and FC-BCz-PQZ in films exhibited large blueshifts of 30 nm and 15 nm compared to those in toluene solution, which are located at 471 nm and 491 nm,

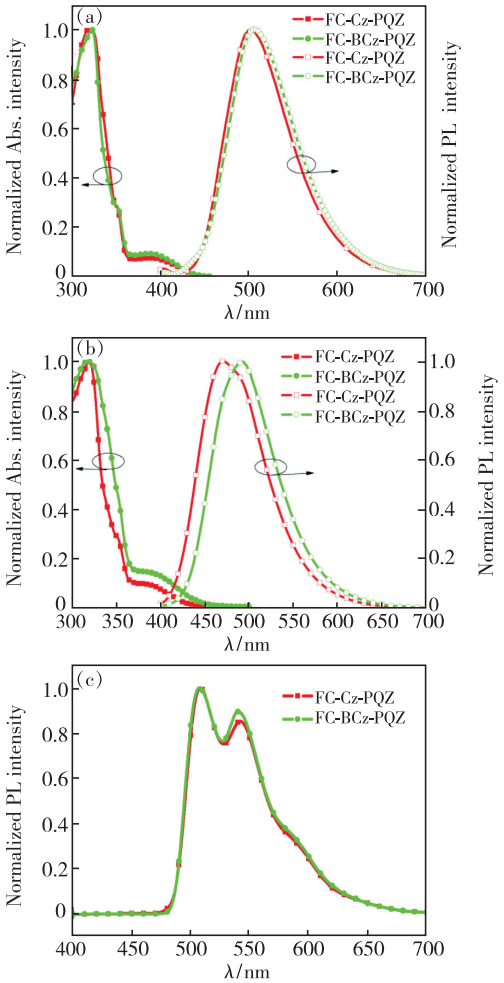

Fig. 2 UV-visible absorption and fluorescence spectra of FC-Cz-PQZ and FC-BCz-PQZ in toluene solvents (a), and in films (b). (c) Phosphorescence spectra of FC-Cz-PQZ and FC-BCz-PQZ.

respectively. These large blueshifts of FC-Cz-PQZ and FC-BCz-PQZ in films are attributed to an increase in the spatial structure of the molecule caused by FC. The large spatial structure and torsion angle prevented intermolecular packing, weakened intermolecular interaction and created blueshifts, which avoided quenching of exciton concentration and contributed to the improvement of luminous efficiency.

The optical band gap (E_g) of FC-Cz-PQZ and FC-BCz-PQZ was calculated to be 3.03 eV and 2.93 eV, respectively, from the intersection between the absorption and emission spectra in films. Furthermore, the triplet energy (E_T) estimated from the phosphorescence spectrum in toluene at 77 K was 2.58 eV for FC-Cz-PQZ and 2.57 eV for FC-BCz-PQZ, suggesting that the bridge benzene has no effect on the triplet state.

3.3 Theoretical Investigation and Energy Level Structure

In order to further understand the electronic properties of FC-Cz-PQZ and FC-BCz-PQZ at the molecular level, frontier molecular orbital energy levels were calculated at the B3LYP/6-31G level by density functional theory. As shown in Fig. 3, the LUMO levels of FC-Cz-PQZ and FC-BCz-PQZ were both mainly located at PQZ. On the other hand, HOMO levels of the two compounds were distributed among the electron-donating FC and carbazole and the 9-phenyl-9*H*-carbazole moiety. Besides, the torsion angle between the carbazole group and the FC of FC-Cz-PQZ and between the 9-phenyl-9*H*-carbazole and the FC of FC-BCz-PQZ was 120.93° and 36.94°, respectively. The smaller twist angle in FC-BCz-PQZ compared with FC-Cz-PQZ was due to the introduction of bridge benzene, expansion of the conjugation between FC and carbazole and reduction of steric hindrance. The FC moiety contributed to the effective separation of the electron density of the HOMOs and LUMOs, which induces a high E_T. Besides, the desirable separation of the HOMOs and LUMOs was beneficial for the transporting balance of holes and electrons.

The HOMO energy levels of FC-Cz-PQZ and FC-BCz-PQZ were measured by IPS. As shown in

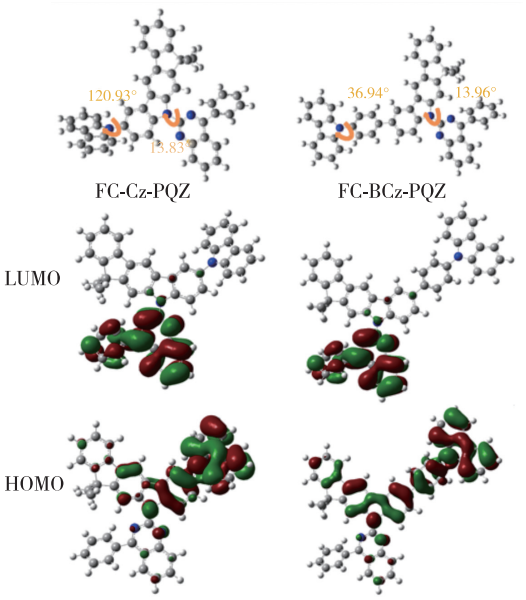

Fig. 3　Molecular orbital surface of the HOMO and LUMO levels of FC-Cz-PQZ and FC-BCz-PQZ

Fig. 4, the E_{HOMO} of FC-Cz-PQZ and FC-BCz-PQZ was 5.75 eV and 5.68 eV, respectively. The HOMO energy level of FC-BCz-PQZ was higher compared with that of FC-Cz-PQZ, which had bigger conjugation due to the FC and carbazole groups with a bridge benzene connection between them. The optical E_g of

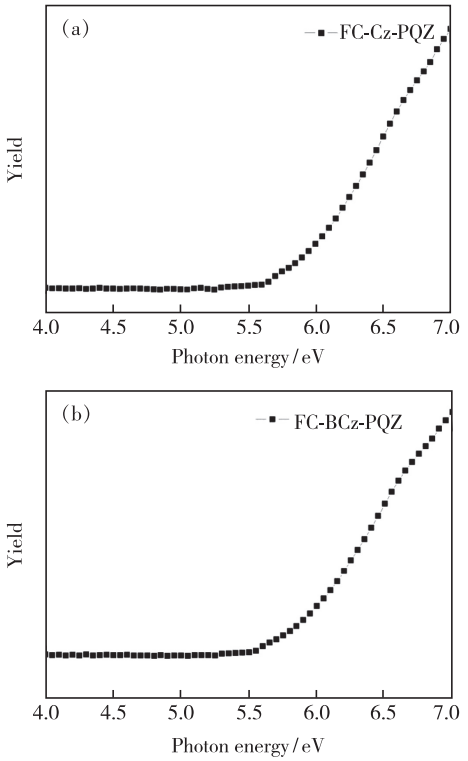

Fig. 4　Energy levels of FC-CZ-PQZ and FC-BCz-PQZ were measured by ionization photoelectron spectrograph

FC-Cz-PQZ and FC-BCz-PQZ was calculated to be 3.03 eV and 2.93 eV, respectively. According to the formula LUMO = HOMO + E_g, the LUMO energy level of FC-Cz-PQZ and FC-BCz-PQZ was 2.72 eV and 2.75 eV, respectively. The LUMOs of the two compounds are nearly identical due to their similar A units.

3.4 Carrier Transport Properties

In order to verify the bipolar charge transport capabilities of FC-Cz-PQZ and FC-BCz-PQZ, hole-only(HOD) and electron-only(EOD) devices were fabricated with the following configurations: ITO/molybdenum oxide(MoO_3, 3 nm)/4,4′-bis[*N*-(1-naphthyl)-*N*-phenylamino]biphenyl(NPB, 25 nm)/tris(4-(9*H*-carbazol-9-yl)phenyl)amine (TCTA, 8 nm)/host(20 nm)/MoO_3(3 nm)/Al(HOD) and ITO/host(20 nm)/1,3,5-tris(1-phenyl-1*H*-benzo[d]imida-ole-2-yl)benzene(TPBi, 45 nm)/lithium fluoride(LiF, 0.5 nm)/Al(EOD). In Fig. 5, it can be seen that FC-Cz-PQZ and FC-BCz-PQZ exhibited different voltage *versus* current density(*V*-*J*) curves in HOD and EOD. The hole current density of FC-Cz-PQZ was higher than the electron current density, which led to unbalanced bipolar transporting ability. Besides, FC-BCz-PQZ exhibited similar hole current and electron current densities in comparison

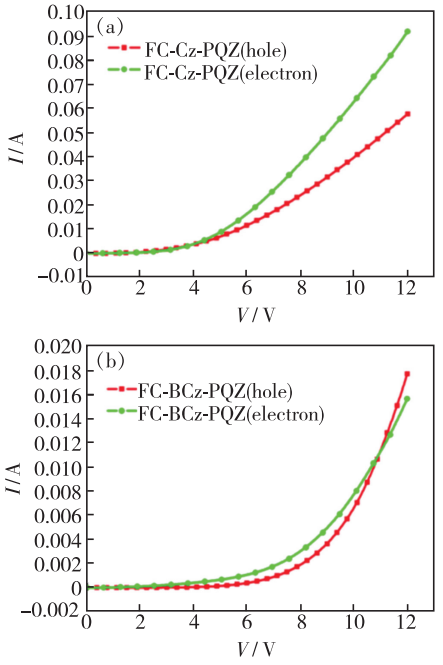

Fig. 5 Current density-voltage curves of HOD(a) and EOD(b)

with FC-Cz-PQZ, indicating its good and balanced carrier mobility that provided the evidence to support its better EL performance.

3.5 Electroluminescence of PHOLEDs

In order to evaluate the performance of FC-Cz-PQZ and FC-BCz-PQZ as host materials, three PhOLEDs with the following configuration were fabricated: ITO/MoO_3(3 nm)/NPB(25 nm)/TCTA(8 nm)/host:Ir(piq)$_2$(acac)(20 nm, 4%)/TPBi(45 nm)/

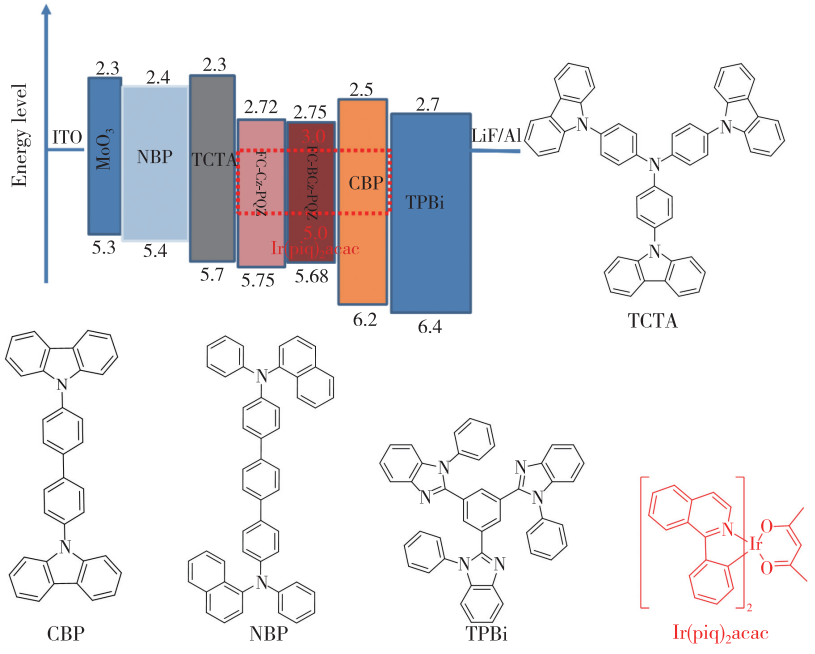

Fig. 6 The energy level diagram of the materials in devices

LiF(1 nm)/Al(100 nm). The emitting layer was composed of 4% $Ir(piq)_2(acac)$ doped into the host materials (*i. e.* FC-Cz-PQZ in device A, FC-BCz-PQZ in device B and CBP in device C). ITO and LiF/Al were used as the anode and cathode, respectively. MoO_3 was employed as the hole injection layer, NPB served as the hole-transporting layer, TCTA was used as the electron-blocking layer and TPBi was employed as the hole-blocking layer and electron-transporting layer. The device and the related HOMO and LUMO energy levels of these materials in PhOLEDs are displayed in Fig. 6. As shown in Tab. 2, the turn-on voltages (V_{on}) of devices A and B are both 2.7 eV, which are slightly lower than V_{on} of device C (3.0 V). It is attributed to a smaller hole injection energy barrier (*i. e.* 0.05 eV in device A and 0.02 eV in device B) between E_{HOMO} of host and E_{HOMO} of TCTA in devices A and B than that in device C (0.5 eV). The maximum luminance of devices A, B and C was 24 600, 24 380, 21 480 cd/m^2, respectively. Compared with FC-Cz-PQZ, FC-BCz-PQZ had more balanced carrier transporting ability. Hence, in device B, the holes and electrons could recombine into excitons in the emission layer with high efficiency, resulting in higher luminance than in device A. Among the three PhOLEDs, device B exhibited the highest device efficiency with the maximum current efficiency (η_c), maximum power efficiency (η) and maximum EQE of 13.5 cd/A, 14.2 lm/W and 14.8%, owing

Tab. 2　Characteristics of OLEDs with FC-Cz-PQZ and FC-BCz-PQZ host materials

Device	Compound	V_{on}[a]/V	L_{max}/(cd·m^{-2})	$\eta_{c\ max}$[b]/(cd·A^{-1})	$\eta_{p\ max}$[c]/(lm·W^{-1})	EQE_{max}[d]/%	CIE (x, y)
A	FC-Cz-PQZ	2.7	24 600	10.9	11.5	11.3	(0.67, 0.32)
B	FC-BCz-PQZ	2.7	24 380	13.5	14.2	14.8	(0.67, 0.32)
C	CBP	3.0	21 480	10.7	9.8	11.7	(0.68, 0.32)

[a] Turn-on voltage estimated at a brightness of 1 cd/m^2. [b] The maximum current efficiency. [c] The maximum power efficiency. [d] The maximum external quantum efficiency.

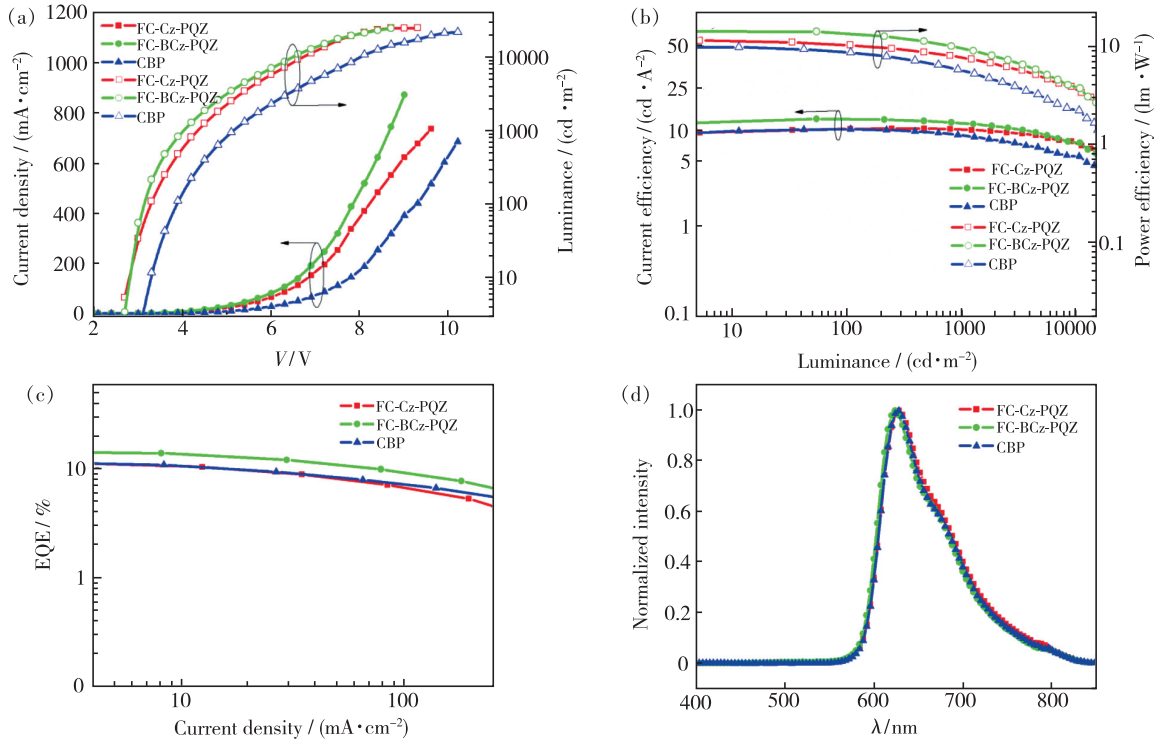

Fig. 7　(a) Current density-voltage-luminance (*J-V-L*) characteristics. (b) Current and power efficiency. (c) External quantum efficiency (EQE) *versus* current density. (d) EL spectra at 4 V of red PhOLEDs.

to the better bipolar charge transporting ability of FC-BCz-PQZ compared with that of FC-Cz-PQZ. As shown in Fig. 7(d), the three PhOLEDs exhibited nearly identical EL spectra with red emission peaks. The devices only display the typical emission spectra from $Ir(piq)_2(acac)$ at 628 nm and 624 nm without any other peaks, indicating full exciton energy utilisation.

4 Conclusion

In summary, two bipolar host materials, FC-Cz-PQZ and FC-BCz-PQZ, were synthesised and characterised. The fabricated red PhOLEDs using FC-Cz-PQZ and FC-BCz-PQZ as host and $(piq)_2Ir(acac)$ as guest emitter realised high device performance. Compared with FC-Cz-PQZ, FC-BCz-PQZ demonstrated its promising potential as a desirable host material for red PhOLEDs with a high T_d of 480 ℃. The red PhOLEDs based on FC-BCz-PQZ host material with the structure of ITO/MoO_3/NPB/TCTA/host: $Ir(piq)_2(acac)$ (4%)/TPBi/LiF/Al showed good electroluminescence performance and balanced hole-electron transport property with low turn-on voltage and maximum current, power and EQE of 13.5 cd/A, 14.2 lm/W and 14.8%, respectively. We believe that this work could shed light on promising bipolar host materials with rational connection of quinazoline derivatives.

Supplementary Information and Response Letter are available for this paper at: http://cjl.lightpublishing.cn/thesisDetails#10.37188/CJL.20210397.

References:

[1] TANG C W, VANSLYKE S A. Organic electroluminescent diodes [J]. *Appl. Phys. Lett.*, 1987, 51(12): 913-915.

[2] BALDO M A, O'BRIEN D F, YOU Y, *et al.* Highly efficient phosphorescent emission from organic electroluminescent devices [J]. *Nature*, 1998, 395(6698): 151-154.

[3] D'ANDRADE B W, FORREST S R. White organic light-emitting devices for solid-state lighting [J]. *Adv. Mater.*, 2004, 16(18): 1585-1595.

[4] LIU X Y, LIANG F, YUAN Y, *et al.* Utilizing 9,10-dihydroacridine and pyrazine-containing donor-acceptor host materials for highly efficient red phosphorescent organic light-emitting diodes [J]. *J. Mater. Chem.* C, 2016, 4(33): 7869-7874.

[5] SASABE H, TOYOTA N, NAKANISHI H, *et al.* 3,3′-bicarbazole-based host materials for high-efficiency blue phosphorescent OLEDs with extremely low driving voltage [J]. *Adv. Mater.*, 2012, 24(24): 3212-3217.

[6] CHIDIRALA S, ULLA H, VALABOJU A, *et al.* Pyrene-oxadiazoles for organic light-emitting diodes: triplet to singlet energy transfer and role of hole-injection/hole-blocking materials [J]. *J. Org. Chem.*, 2016, 81(2): 603-614.

[7] MA Y G, ZHANG H Y, SHEN J C, *et al.* Electroluminescence from triplet metal-ligand charge-transfer excited state of transition metal complexes [J]. *Synth. Met.*, 1998, 94(3): 245-248.

[8] XU H, CHEN R F, SUN Q, *et al.* Recent progress in metal-organic complexes for optoelectronic applications [J]. *Chem. Soc. Rev.*, 2014, 43(10): 3259-3302.

[9] HUANG H, WANG Y X, ZHUANG S Q, *et al.* Simple phenanthroimidazole/carbazole hybrid bipolar host materials for highly efficient green and yellow phosphorescent organic light-emitting diodes [J]. *J. Phys. Chem.* C, 2012, 116(36): 19458-19466.

[10] TING H C, CHEN Y M, YOU H W, *et al.* Indolo[3,2-*b*] carbazole/benzimidazole hybrid bipolar host materials for highly efficient red, yellow, and green phosphorescent organic light emitting diodes [J]. *J. Mater. Chem.*, 2012, 22(17): 8399-8407.

[11] HUANG J J, LEUNG M K, CHIU T L, *et al.* Novel benzimidazole derivatives as electron-transporting type host to achieve highly efficient sky-blue phosphorescent organic light-emitting diode (PHOLED) device [J]. *Org. Lett.*, 2014, 16(20): 5398-5401.

[12] ZHUANG J Y, SU W M, LI W F, *et al.* Configuration effect of novel bipolar triazole/carbazole-based host materials on the performance of phosphorescent OLED devices [J]. *Org. Electron.*, 2012, 13(10): 2210-2219.

[13] SHIH P I, CHIEN C H, CHUANG C Y, *et al.* Novel host material for highly efficient blue phosphorescent OLEDs [J]. *J.*

Mater. Chem., 2007,17(17):1692-1698.

[14] KAUTNY P,WU Z B,EICHELTER J,*et al.* Indolo[3,2,1-*jk*] carbazole based planarized CBP derivatives as host materials for PhOLEDs with low efficiency roll-off [J]. *Org. Electron.*, 2016,34:237-245.

[15] SEO J A,JEON S K,LEE J Y. Acridine derived stable host material for long lifetime blue phosphorescent organic light-emitting diodes [J]. *Org. Electron.*, 2016,34:33-37.

[16] XIE Y M,CUI L S,LIU Y,*et al.* Efficient blue/white phosphorescent organic light-emitting diodes based on a silicon-based host material *via* a direct carbon-nitrogen bond [J]. *J. Mater. Chem.* C, 2015,3(20):5347-5353.

[17] PATIL B N,LADE J J,VADAGAONKAR K S,*et al.* Pyrrolo [1,2-a] quinoxaline-based bipolar host materials for efficient red phosphorescent OLEDs [J]. *ChemistrySelect*, 2018,3(35):10010-10018.

[18] TAVGENIENE D,KRUCAITE G,BARANAUSKYTE U,*et al.* Phenanthro [9,10-*d*] imidazole based new host materials for efficient red phosphorescent OLEDs [J]. *Dyes Pigm.*, 2017,137:615-621.

[19] WANG F,ZHAO Y P,XU H X,*et al.* Two novel bipolar hosts based on 1,2,4-triazole derivatives for highly efficient red phosphorescent OLEDs showing a small efficiency roll-off [J]. *Org. Electron.*, 2019,70:272-278.

[20] WANG H,LIU Y W,HU W J,*et al.* Novel spironaphthalenone-based host materials for efficient red phosphorescent and thermally activated delayed fluorescent OLEDs [J]. *Org. Electron.*, 2018,61:376-382.

[21] XU H X,ZHANG D,ZHAO Y P,*et al.* Novel donor-acceptor-donor hosts for green and red phosphorescent OLEDs achieving high device efficiency and low efficiency roll-off [J]. *Dyes Pigm.*, 2020,180:108491-1-6.

[22] LIU X Y,MA Y Y,ZHANG W J,*et al.* A novel linking strategy of using 9,10-dihydroacridine to construct efficient host materials for red phosphorescent organic light-emitting diodes [J]. *Chem. Eur. J.*, 2018,24(45):11755-11762.

[23] KUMAR S,LI D,WANG Y K,*et al.* One-shot triphenylamine/phenylketone hybrid as a bipolar host material for efficient red phosphorescent organic light-emitting diodes [J]. *Synth. Met.*, 2019,254:42-48.

[24] BEZVIKONNYI O,GRYBAUSKAITE-KAMINSKIENE G,VOLYNIUK D,*et al.* 3,3′-Bicarbazole-based compounds as bipolar hosts for green and red phosphorescent organic light-emitting devices [J]. *Mater. Sci. Eng.* B, 2020,261:114662-1-8.

[25] BEZVIKONNYI O,GUDEIKA D,VOLYNIUK D,*et al.* Pyrenyl substituted 1,8-naphthalimide as a new material for weak efficiency-roll-off red OLEDs:a theoretical and experimental study [J]. *New J. Chem.*, 2018,42(15):12492-12502.

[26] CHEN X,ZHUANG X M,WANG Z Y,*et al.* A multifunctional bipolar host material based on phenanthroimidazole for efficient green and red PhOLEDs with low turn-on voltage [J]. *Org. Electron.*, 2019,69:85-91.

[27] CHEN Y,WEI X,CAO J,*et al.* Novel bipolar indole-based solution-processed host material for efficient green and red phosphorescent OLEDs [J]. *ACS Appl. Mater. Interfaces*, 2017,9(16):14112-14119.

[28] FENG Z L,GAO Z X,QU W S,*et al.* Rational design of quinoxaline-based bipolar host materials for highly efficient red phosphorescent organic light-emitting diodes [J]. *RSC Adv.*, 2019,9(19):10789-10795.

[29] LADE J,LEE N Y,PATIL B,*et al.* Novel benzothiadiazine 1,1-dioxide based bipolar host materials for efficient red phosphorescent organic light emitting diodes [J]. *Org. Electron.*, 2021,92:106104-1-9.

[30] HAN C M,ZHANG Z,DING D X,*et al.* Dipole-dipole interaction management for efficient blue thermally activated delayed fluorescence diodes [J]. *Chem*, 2018,4(9):2154-2167.

[31] HAN C M,YANG W B,XU H. Asymmetrically phosphorylated carbazole host for highly efficient blue and white thermally activated delayed fluorescence diodes [J]. *Chem. Eng. J.*, 2020,401:126049-1-8.

[32] HAN C M,ZHANG J,MA P,*et al.* Host engineering based on multiple phosphorylation for efficient blue and white TADF organic light-emitting diodes [J]. *Chem. Eng. J.*, 2021,405:126986.

[33] LI H H,WANG Y Z,YU L,*et al.* V-shaped triazine host featuring intramolecular non-covalent interaction for highly efficient white electroluminescent devices [J]. *Chem. Eng. J.*, 2021,425:131487.

[34] 孙军,张玉祥,赵卫华,等. 基于 7-(9H-carbazol-9-yl)-N,N-diphenyl-9,9′-spirobi [fluoren]-2-amine 主体材料的高效红色电致磷光器件 [J]. 发光学报, 2014,35(3):327-331.
SUN J,ZHANG Y X,ZHAO W H,*et al.* Highly efficient red electrophosphorescent devices based on 7-(9H-carbazol-9-yl)-N,N-diphenyl-9,9′-spirobi [fluoren]-2-amine host material [J]. *Chin. J. Lumin.*, 2014,35(3):327-331. (in Chinese)

[35] PATIL B,LADE J,CHIOU S S,*et al.* Carbazole/triphenylamine-cyanobenzimidazole hybrid bipolar host materials for green

phosphorescent organic light-emitting diodes [J]. *Org. Electron.*, 2021, 92: 106090-1-14.

[36] KIM S M, YUN J H, HAN S H, *et al.* Novel aromatic extended carbazoles as a chemical platform of bipolar hosts for improved lifetime in phosphorescent organic light-emitting diodes [J]. *J. Ind. Eng. Chem.*, 2020, 84: 217-225.

[37] LIPUNOVA G N, NOSOVA E V, CHARUSHIN V N, *et al.* Functionalized quinazolines and pyrimidines for optoelectronic materials [J]. *Curr. Org. Synth.*, 2018, 15(6): 793-814.

[38] LI B W, WANG Z H, SU S J, *et al.* Quinazoline-based thermally activated delayed fluorecence for high-performance OLEDs with external quantum efficiencies exceeding 20% [J]. *Adv. Opt. Mater.*, 2019, 7(9): 1801496-1-8.

[39] HUA M M, XU Q H, JIANG Y X, *et al.* Bipolar carbazole/quinoxaline-based host materials for efficient red PhOLEDs [J]. *Dyes Pigm.*, 2018, 150: 185-192.

凌乾坤(1994 -),男,河南商丘人,硕士研究生,2019年于河南工程学院获得学士学位,主要从事应用于有机发光二极管的红光磷光双极性主体材料的研究。
E-mail: 1192142380@qq.com

王华(1977 -),男,山西平定县人,博士,教授,博士生导师,2007年于太原理工大学获得博士学位,主要从事有机半导体光电材料与器件的研究。
E-mail: wanghua001@tyut.edu.cn

陈志宽(1967 -),男,四川绵阳人,博士,教授,博士生导师,1995年于北京大学获得博士学位,主要从事有机光电材料的设计与合成、材料光电特性及薄膜特性、材料的器件特性及其与材料结构的构效关系及器件制程、器件物理、器件集成等方面的研究。
E-mail: zkchen@lumilan.cn

李天保(1974 -),男,山西临县人,博士,教授,博士生导师,2008年于太原理工大学获得博士学位,主要从事光电半导体器件及制备工艺的研究。
E-mail: litianbao@tyut.edu.cn